ELSEVIER

Imazalil–cyclomaltoheptaose (β-cyclodextrin) inclusion complex: preparation by supercritical carbon dioxide and ^{13}C CPMAS and ^{1}H NMR characterization

Simona Lai, Emanuela Locci, Alessandra Piras, Silvia Porcedda, Adolfo Lai,*
Bruno Marongiu

Dipartimento di Scienze Chimiche, Università di Cagliari, Cittadella Universitaria di Monserrato, Strada Statale 554 Bivio per Sestu, 09042 Monserrato (CA), Italy

Abstract

An inclusion complex between imazalil (IMZ), a selected fungicide, and cyclomaltoheptaose (β-cyclodextrin, βCD) was obtained using supercritical fluid carbon dioxide. The best preparation conditions were determined, and the inclusion complex was investigated by means of ^{1}H NMR spectroscopy in aqueous solution and ^{13}C CPMAS NMR spectroscopy in the solid state. Information on the geometry of the βCD/IMZ complex was obtained from ROESY spectroscopy, while the dynamics of the inclusion complex in the kilohertz range was obtained from the proton spin-lattice relaxation times in the rotating frame, $T_{1\rho}$ (^{1}H).
© 2003 Elsevier Ltd. All rights reserved.

Keywords: Imazalil; Cyclomaltoheptaose; β-Cyclodextrin; Inclusion complexes; Supercritical fluid carbon dioxide; ^{1}H NMR spectroscopy; ^{13}C CPMAS NMR spectroscopy

1. Introduction

Imazalil (IMZ) is one of the few fungicides permitted in the post-harvest treatment of fruits, vegetables and ornamentals.[1–3] However, the fact that IMZ is poorly soluble in water (0.018 g/100 mL) remarkably reduces its bioavailability and effectiveness and consequently its antifungal activity in agricultural applications.

In order to improve the solubility of IMZ in water and reduce its toxicity, especially when handled by operators, IMZ has recently been microencapsulated in cyclomaltoheptaose (β-cyclodextrin, hereafter, βCD) by easy preparation in water of a stable inclusion complex, βCD/IMZ.[4] βCD is an oligosaccharide matrix convenient and commercially acceptable in post-harvest treatments, since it does not require agrochemical inputs as large as those required in field treatments. Both the

structure and molecular size of IMZ fit the βCD cavity well, giving rise to significant electronic and Van der Waals interactions. The antifungal activity of the βCD/IMZ complex against *Penicillium digitatum* and *P. italicum* was studied by in vitro and in vivo tests in the post-harvest treatment of citrus fruit, and encouraging results were obtained.[4]

Several preparation methods in solution are generally available to prepare βCD–drug inclusion complexes.[5,6] Some of these are suitable for the production of complexes on the laboratory scale, whereas others can be scaled up for industrial production. However, many of these methods are time consuming and need multi-stage processing, involving the evaporation of large volumes of solvent, which is often found in the complex as a residue.

In this work, in order to avoid these disadvantages, and in particular to improve the purity of the product, the βCD/IMZ inclusion complex was prepared using the supercritical fluid carbon dioxide technique (SCF), which is a well-known environmentally sustainable method.[7–12]

* Corresponding author. Tel.: +39-070-6754389; fax: +39-070-6754388.

E-mail address: adolfo@mvcch3.unica.it (A. Lai).

The βCD/IMZ inclusion complex was characterized using ^{1}H NMR spectroscopy in aqueous solution and ^{13}C CPMAS NMR spectroscopy in the solid state. As a matter of fact, these techniques give complementary information on the structural properties of the host and guest molecules in the inclusion complex. In addition, the spin-diffusion processes characterising the inclusion complex were investigated by analysing the proton spin-lattice relaxation times in the rotating frame, $T_{1\rho}$ (^{1}H), in the CPMAS ^{13}C NMR spectra of the solid complex.

2. Results and discussion

2.1. Preparation of βCD/IMZ by SCF

In order to prepare the βCD/IMZ inclusion complex by SCF with a good complexation efficiency (see Section 3), the experimental conditions were optimised by testing several values of the process thermodynamic parameters, such as temperature, pressure, and βCD–IMZ–CO_2 contact time.

Fig. 1a shows the variation of the complexation efficiency as a function of the βCD–IMZ–CO_2 contact time. In these experiments, the temperature was fixed at 65 °C, since at lower temperatures IMZ is a solid (mp 55 °C), while the pressure was fixed at 150 and 200 bar, which are pressure values that allow for the formation of relevant quantities of complex. As shown, the com-
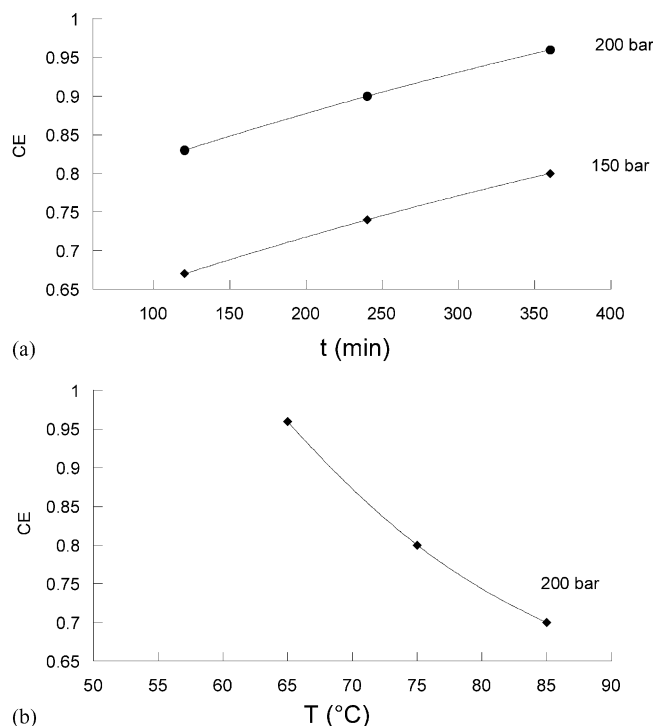

(a)

(b)

Fig. 1. Complexation efficiency (CE) of βCD–IMZ as a function of: (a) contact time (at 65 °C and 200 bar); and (b) temperature (at 6 h contact time and 200 bar).

plexation efficiency increases at increasing contact times and pressures. At a contact time of 6 h and a pressure of 200 bar, an equimolar host–guest ratio is reached similar to the one previously found for the βCD/IMZ complex prepared in water.[4] These parameters represent the best experimental conditions to obtain the highest host–guest molar ratio. As a matter of fact, as shown in Fig. 1b, on increasing the temperature the complexation efficiency is reduced, due to a decrease in density and consequently in the solvating power of the supercritical CO_2.
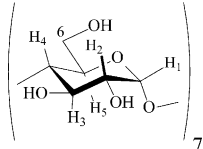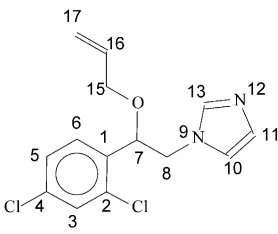
2.2. ^{1}H NMR spectra

The ^{1}H NMR resonances of the βCD, IMZ and the βCD/IMZ inclusion complex in D_2O are reported in Table 1. The βCD resonances were assigned according to a previous NMR investigation,[4] whereas those of IMZ resonances were obtained from TOCSY NMR experiment. As already observed for the βCD/IMZ inclusion complex prepared in water,[4] the H-3 and H-5 signals are shifted about 0.1 ppm upfield from the free βCD. This is taken as the evidence of complex formation, since they point into the hydrophobic cavity of βCD and are thus directly involved in the host–guest interactions. In addition, changes in chemical shift and splitting of the signals of the guest molecule are observed. In particular, the resonances of the H-10 and H-13 of IMZ split into two signals that are indicative of two distinct arrangements of the imidazole ring. This can be attributed to the presence of two βCD/IMZ diastereomeric forms originating from the stereogenic centre of IMZ (C-7) and the chiral cavity of βCD.

The ^{1}H NMR spectrum of a βCD/IMZ physical mixture was also recorded and compared with that of the βCD/IMZ inclusion complex (Fig. 2). As shown, the signals of the IMZ protons in the physical mixture are not detected owing to the very low solubility of the free IMZ in water, while they are present in the spectrum of the inclusion complex, confirming that IMZ is encaged in the βCD cavity.

In order to gain information on the geometry of the inclusion complex, NOESY and ROESY experiments were performed. While NOESY experiments did not show any cross-peak, due to unfavourable molecular correlation times, ROESY experiments showed several cross-peaks between βCD and IMZ protons. In particular, cross-peaks have been easily recognized between H-3 and H-5 of βCD, and H-3, H-5 and/or H-6 of IMZ, indicating that this region of the phenyl ring of IMZ is encaged in the βCD cavity. Interestingly, the intensity of the cross-peak between H-3 of βCD and H-5 and/or H-6 of IMZ is much higher than that of the cross-peak between H-5 of βCD and H-5 and/or H-6 of IMZ (and also than that of the remaining cross-peaks). Thus, it is likely that H-3 of βCD is in dipolar contact with both H-

Table 1
^{1}H NMR chemical shifts (δ) of βCD, IMZ and βCD/IMZ in D$_2$O

	Proton type	δ (ppm)	
		Free	Inclusion complex
βCD	H-1	5.01	5.00
	H-2	3.59	3.58
	H-3	3.91	3.80
	H-4	3.53	3.52
	H-5	3.80	3.71
	H-6	3.82	3.82
IMZ	H-13	7.57	7.58
	H-3	7.51	7.54
	H-6	7.31	7.34
	H-5	7.22	
	H-10	7.04	7.07/7.10
	H-11	6.93	6.96
	H-16	5.78	5.71
	H-15	5.18	5.18
	H-7	5.15	5.12
	H-8	4.32	4.28
	H-17	3.95/3.84	3.99/3.86

5 and H-6 of IMZ, contrary to H-5 of βCD, which is in dipolar contact only with H-5 of IMZ. These results suggest that the phenyl ring of IMZ enters into the βCD cavity from the wider rim with C1–4 deeply inserted into the cavity.

Cross-peaks of low intensity were also found between H-6 of βCD and H-8 and H-10 of IMZ. However, since H-6 is largely overlapped by the resonance H-3 of βCD and since the former is likely to be strongly *J*-coupled with H-5 (βCD), no analysis has been made.

2.3. ^{13}C CPMAS NMR spectra

Fig. 3 shows the solid-state ^{13}C CPMAS NMR spectra of the βCD (a), IMZ (b), βCD–IMZ inclusion complex (c) and βCD/IMZ physical mixture (d). The assignment of the βCD resonances was made following a previous NMR investigation,[13] while the IMZ resonances were attributed from the analysis of the coupled and decoupled ^{13}C NMR spectra in CDCl$_3$ (see Table 2).

As can be observed, the spectrum of βCD has a relatively poor resolution, due to the partial hydration of the sample.[14] It has already been shown that the appearance of multiple resonances for atoms C-2, C-3, C-5, C-4, and C-6 of the glucopyranose unit is an indication of the coexistence of different structural arrangements.[13] Similar observations can be made by analysing the signals of the βCD/IMZ physical mixture, while the spectrum of the inclusion complex shows

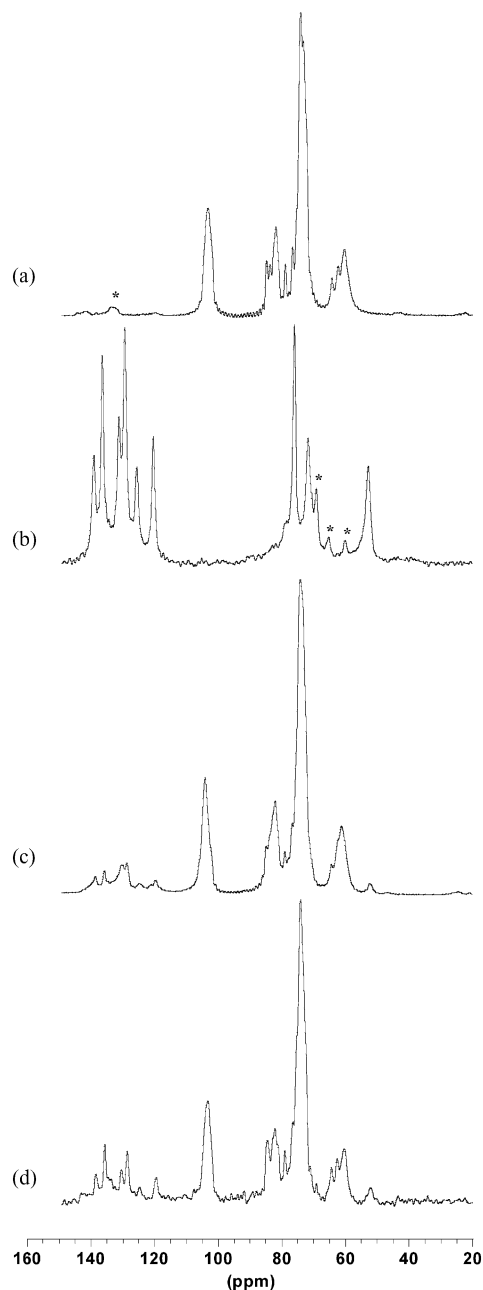Fig. 2. ^{1}H NMR spectra in aqueous solution of: (a) βCD/IMZ inclusion complex; and (b) βCD–IMZ physical mixture [1:1 (mole/mole) solid mixture was dissolved in D$_2$O]. The same number of scans was recorded in each spectrum.

Fig. 3. ^{13}C CPMAS NMR spectra of: (a) βCD; (b) IMZ; (c) βCD–IMZ inclusion complex; and (d) 1:1 (mole/mole) βCD–IMZ physical mixture (recorded using an 8-ms contact time to enhance the signal-to-noise ratio of the free IMZ resonances). The asterisk indicates a spinning side band.

changes in intensity and chemical shift of the βCD and IMZ signals after complexation. In particular, each set of multiple resonances of the carbons of the glucose units tends to converge to a single peak, suggesting that the glucose units adopt a more symmetrical conformation in the complex. As to IMZ, changes in chemical shift and a marked broadening of all signals are observed, following the encaging of βCD into the hydrophobic cavity. It is worthwhile to note that several

Table 2
^{13}C NMR chemical shifts (δ) of βCD, IMZ and βCD/IMZ

	Carbon type	δ (ppm)	
		Free	Inclusion complex
	C-1	103.1	104.1
	C-4	84.9	84.8
		84.0	
		82.0	82.1
βCD		79.0	79.0
	C-2-C-3-C-5	76.8	76.8
		75.5	
		74.3	74.2
	C-6	64.4	64.3
		62.5	
		60.5	61.2
	C-1, C-13	139.1	138.6
	C-4, C-16	136.5	135.8
	C-2	131.2	130.3
	C-3, C-11	129.4	128.7
IMZ	C-5, C-6	125.7	124.8
	C-10, C-17	120.4	121.1
			119.7
	C-7	76.1	nd
	C-15	71.7	nd
	C-8	52.8	52.4

Table 3
Spin-lattice relaxation times in the rotating frame, $T_{1\rho}$ (^{1}H), of the βCD, IMZ and βCD–IMZ

	Carbon type	$T_{1\rho}$ (^{1}H) (ms)	
		Free	Inclusion complex
	C-1	3.2	4.0
βCD	C-4	2.8	3.8
	C-2-C-3-C-5	3.2	3.9
	C-6	3.1	4.1
	C-1, C-13	139	3.7
	C-4, C-16	114	3.3
	C-2	143	4.5
	C-3, C-11	154	5.4
IMZ[a]	C-5, C-6	91	5.0
	C-10, C-17	170	-
	C-7	180	-
	C-15	169	-
	C-8	164	5.4

The standard deviations from fit were not higher than 10%. It must be pointed out that the long T_1 of free IMZ prevented an accurate measurement of $T_{1\rho}$ (^{1}H), which should be taken only on a qualitative basis.

resonances of IMZ split up into multiple signals, indicative of a pronounced structural rearrangement of the imidazole and aryl rings.

2.4. Rotating frame ^{1}H NMR relaxation

In order to obtain additive information on the dynamics of the βCD–IMZ complex, we measured the proton relaxation times in the rotating frame, $T_{1\rho}$ (^{1}H), which are sensitive to the motions in the kilohertz range. Averaged over the intrinsic proton relaxation times, this parameter is determined by the ^{1}H spin-diffusion process and therefore depends on the proton–proton intermolecular distance and on the degree of molecular motion of the neighbouring spin reservoirs.[14,15]

The values of $T_{1\rho}$ (^{1}H) for free and complexed βCD and IMZ are shown in Table 3. It can be seen that all the carbon signals of the free βCD have very similar $T_{1\rho}$ (^{1}H) values, indicating that the cyclodextrin moieties are characterised by a single spin reservoir. This is ascribable to the occurrence of domains of very small dimensions homogeneously distributed in the samples.[14,15] It is noteworthy that the $T_{1\rho}$ (^{1}H) of free βCD are longer than those previously reported,[14] due to a partial hydration of our sample as mentioned above. After inclusion of IMZ, the $T_{1\rho}$ (^{1}H)'s of the βCD carbons do not show any significant variation, indicating that the mobility of the sugar rings in the cyclodextrin skeleton of βCD remains practically unchanged.

Unlike the relaxation behaviour of βCD, the pure solid form of IMZ gives rise to much longer $T_{1\rho}$ (^{1}H)'s. On passing from the free IMZ to the complexed form, the $T_{1\rho}$ (^{1}H)'s of all the examined signals decrease remarkably, reaching values similar to those measured for the βCD. Therefore, the fact that the carbon atoms of the guest molecules experience a similar efficiency in the spin-diffusion process as that of the host molecule indicates that the complex is characterised by a single spin reservoir common to βCD and IMZ. This result is consistent with the occurrence of a genuine inclusion complex.

In conclusion, the complexation efficiency in the preparation of the βCD–IMZ complex by the SCF technique is similar to that found for the inclusion complex prepared in water.[4] Furthermore, compared to the latter technique, SCF has important advantages, since it provides an eco-sustainable method to produce βCD–IMZ with no exogenous residue, which also avoids the problems related to solvent evaporation. The combined use of liquid-state ^{1}H NMR and solid-state ^{13}C NMR spectroscopies, together with measurements of proton relaxation times in the rotating frame, afforded the inclusion complex to be efficaciously characterised.

3. Experimental

3.1. General

βCD (CAVAMAX ®7 PHARMA) was obtained from Wacker–Chemie Italia SpA and used as received; CO_2 (purity 99%) was supplied by SIO (Società Italiana Ossigeno, Cagliari, Italy), while IMZ (97%) was purchased from Dr Ehrenstorfer (Augsburg, Germany) and used without further purification.

3.2. SCF apparatus

βCD–IMZ inclusions were performed in a SCF laboratory apparatus, equipped with a thermostatted 400 cm^3 autoclave and supercritical CO_2 pressurized by a high-pressure diaphragm pump (Lewa, model EL 1) with a maximum capacity of 6 kg/h, pumping liquid CO_2 at the chosen pressure. Temperatures and pressures along the extraction apparatus were respectively measured by thermocouple and Bourdon-tube test gauges. Pressure was regulated by high-pressure valves under manual control.[16]

The apparatus was used in the batch mode. About 20 g of βCD with IMZ at a molar ratio of 1:2.5 were loaded into the autoclave, which was then thermostatted and pressurized with CO_2 at fixed pressure and contact time. Then a rapid drop in pressure allowed the CO_2 to vaporize and separate the solid deprived of solvent.

Although an excess of guest molecule was used in all the preparations by SFC, only an equimolar guest–host ratio was achieved. The complexation efficiency was defined as the [βCD]:[IMZ] molar ratio in aqueous solution of the inclusion complex and was determined via integration of the ^{1}H NMR signals of the host and the guest molecules (spectra not shown).

3.3. ^{1}H NMR and solid-state ^{13}C NMR experiments

The ^{1}H and ^{13}C NMR spectra were recorded at $T = 25.0 \pm 0.1$ °C on a Varian 400 Unity Inova spectrometer operating at nominal proton frequency of 400 MHz. The ^{1}H NMR spectra of the βCD, IMZ βCD–IMZ inclusion complex and βCD–IMZ physical mixture in D_2O were recorded in 5-mm tubes, using the following experimental conditions: 9 μs pulse (90°), 8.7 s repetition time and a spectral width of 6000 Hz. A total of 64 scans were recorded for each spectrum. The residual water signal was suppressed by presaturation with low irradiation power.

The NMR pulse sequences used for proton resonance assignments included phase-sensitive total correlated spectroscopy (TOCSY),[17] nuclear Overhauser enhancement spectroscopy (NOESY)[18] and rotating frame nuclear Overhauser enhancement spectroscopy (ROESY). 2D ROESY experiments were performed by

using the pulse sequence proposed by Shaka and co-workers[19] that minimizes the artifacts coming from coherent transfer of magnetization between J-coupled spins. NOESY NMR spectra were recorded with mixing times of 200 ms and 1 s. TOCSY and ROESY NMR spectra were recorded with mixing times of 50 and 250 ms, respectively. In all cases, a 4000 × 4000 Hz window at carrier frequency of 4.74 ppm was obtained acquiring 128 transients with 2k data points along the t_2 axis. Prior to Fourier transformation, free-induction decays were multiplied by a shifted square sine-bell function.

Cross-polarization magic-angle spinning (CPMAS) ^{13}C NMR spectra were recorded at the resonance frequency of 100.57 MHz. A matched set of Hartmann–Hahn conditions were established at the spin-lock field of 38 kHz. The rotor was spun at a rate of 6 kHz, and working at room temperature a contact time of 500 μs was applied to obtain polarization transfer. A recycle delay of 5 s and a 90° pulse of 5.8 μs were used. Chemical shifts of CPMAS spectra were originally obtained with respect to the methylene carbon resonance of solid adamantane, 38.3 ppm with respect to Me$_4$Si, measured before each measurement. Experiments were conducted on 160–180 mg packed into a 7-mm ZrO$_2$ rotor.

The proton relaxation times in the rotating frame $T_{1\rho}$ (^{1}H) were determined from an exponential fit to the decay of the carbon signal as a function of the time before cross-polarization in the range 0.2–400 ms for free IMZ and in the range 0.2–20 ms for the free βCD and the βCD–IMZ inclusion complex.

Acknowledgements

References

1. White-Weithers, N.; Medleau, L. *J. Am. Anim. Hosp. Assoc.* **1995**, *31*, 250–253.
2. Schirra, M.; D'hallewin, G.; Cabras, P.; Angioni, A.; Ben-Yehoshua, S.; Lurie, S. *Postharvest Biol. Technol.* **2000**, *20*, 91–98.
3. Eckert, J. W. *Tree Fruit Postharvest J.* **1995**, *6*, 9–12.
4. Schirra, M.; Delogu, G.; Cabras, P.; Angioni, A.; D'hallewin, G.; Veyrat, A.; Marcos, J. F.; Gonzáles Candelas, L. *J. Agric. Food Chem.* **2002**, *50*, 6790–6797.
5. Szejtli, J. Cyclodextrin technology. In *Topics in Inclusion Science* Cyclodextrin technology; Vol. 8; N.L. Dordrecht Ed; Kluwer Academic Publ: Norwell, MA, 1988; pp 1–450.
6. Hedges, A. R. *Chem. Rev.* **1998**, *98*, 2035–2044.
7. Smith, R. M. *J. Chromatogr. A* **1999**, *856*, 83–115.
8. McHugh, M. A.; Krukonis, V. J. *Supercritical Fluid Extraction Principles and Practice*; 2nd ed.; Butterworth-Heinemann: Boston, MA, 1994; pp 1–512.
9. Charoenchaitrakool, M.; Dehghani, F.; Foster, N. R. *Int. J. Pharm.* **2002**, *239*, 103–112.
10. Van Hees, T.; Piel, G.; Evrard, B.; Otte, X.; Thunus, L.; Delattre, L. *Pharm. Res.* **1999**, *16*, 1864–1870.
11. Kompella, U. B.; Koushik, K. *Crit. Rev. Ther. Drug Carrier Syst.* **2001**, *18*, 173–199.
12. Sunkara, G.; Kompella, U.B., *Drug Deliv. Technol.* **2002**, 2.
13. Lima, S.; Gonçalves, I. S.; Ribeiro-Claro, P.; Pillinger, M.; Lopes, A. D.; Ferreira, P.; Teixeira-Dias, J. J. C.; Rocha, J.; Romão, C. C. *Organometallics* **2001**, *20*, 2191–2197.
14. Crini, G.; Cosentino, C.; Bestini, S.; Naggi, A.; Torri, G.; Vecchi, C.; Janus, L.; Morcellet, M. *Carbohydr. Res.* **1998**, *308*, 37–45.
15. Garbow, J. R.; Gaede, B. J. *J. Agric. Food Chem.* **1992**, *40*, 156–159.
16. De Gioannis, B.; Marongiu, B.; Porcedda, S. *J. Essent. Oil Res.* **2001**, *13*, 240–244.
17. Bax, A.; Davis, D. G. *J. Magn. Reson.* **1985**, *65*, 355–360.
18. Jeener, J.; Meier, B. H.; Bachmann, P.; Ernst, R. R. *J. Chem. Phys.* **1979**, *71*, 4546–4553.
19. Hwang, T.-L.; Shaka, A. J. *J. Magn. Res. B* **1993**, *102*, 155–165.